DEVELOPMENT OF AN ONLINE PARAMETER ESTIMATION CAPABILITY FOR AIRCRAFT

Pierre-Daniel Jameson
Dynamics, Simulation and Control Group, Department of Aerospace Sciences,
Cranfield University, Cranfield, Bedfordshire, MK43 0AL, United Kingdom
p.d.jameson@cranfield.ac.uk

Keywords: *System Identification, Parameter Estimation, Online, Post-manoeuvre*

Abstract

Flight Testing is the best means to determine the flying qualities of aircraft and demonstrate compliance to airworthiness regulations. Furthermore, data recorded in flight can also be used to create mathematical models of the aircraft for further testing and development. These models consist of system parameters known as stability and control derivatives, which are determined from flight and wind tunnel tests by parameter estimation techniques. Aircraft system identification as this field is known can be applied to: create models and data sets for aircraft simulators, design flight control laws for stability augmentation systems, and more recently evaluate UAV's. Incentives to perform such a task in real-time include: developing fault-tolerant aircraft architectures and improved flight test efficiency due to rapid data analysis. This paper addresses the issue related to smoothing and differentiating the necessary data for system identification under the constraints of post-manoeuvre performance. Examples of determining the reduced order models for the SPPO mode of the Cranfield University Jetstream-31 (G-NFLA) and a simulated UAV are presented.

Nomenclature

E	Expectation operator
I	Identity matrix
M	Pitching moment
N	Noise model
V_{TAS}	True Airspeed, (kts)
W	Total normal velocity (m/s)
X	Matrix of regressors
Y	Signal model
b	Wing span, (m)
$b(k)$	Fourier sine series coefficients
f_c	Cut-off frequency (Hz)
g	Signal time history
h	Altitude, (ft)
k	Discrete frequency index
n	Number of discrete points
p	Roll rate, (deg/s)
q	Pitch rate, (deg/s)
r	Yaw rate, (deg/s)
y	Observation vector
z	Measurement vector
0	Null matrix
s	Standard error

Greek letters

α	Angle of attack, (deg)
β	Angle of sideslip, (deg)
ϵ	Equation error
η	Elevator deflection, (deg)
θ	Parameter estimate
$\phi(k)$	Wiener filter weighting

Superscripts

^{T}	Transpose
$\hat{}$	Estimate
$\dot{}$	Derivative with respect to time
$^\circ$	Degrees

Abbreviations

DCC	Data compatibility check
DR	Dutch roll
EE	Equation error
FT	Flight test (ing)
Global	Global Fourier smoothing method
Local	Local polynomial smoothing method
MAC	Mean aerodynamic chord
MTOW	Maximum take-off weight
PID	Parameter identification
SNR	Signal to noise ratio
SPPO	Short period pitching oscillation
SysID	System identification
c.g	Centre of gravity

1 Introduction

During Flight Testing (FT) significant time is dedicated to determining an accurate representative dynamic model of the test aircraft. Such models can be used to validate *a priori* dynamic characteristics that have been established using wind tunnel testing and Computational Fluid Dynamics (CFD) to predict the aircraft's behaviour during the initial design stage. However, in the field of small UAVs their sometimes unconventional and complex shapes may lead to a more feasible option being to determine the dynamic characteristics from the first test flight. Therefore, recent work at Cranfield by Carnduff [1] has concentrated on developing suitable System Identification (SysID) techniques for use with UAVs.

The driving interest behind developing real-time SysID for aircraft stems from the underlining need to maximise useful information about the system's behaviour during a given period of time. Demand for such a capability is necessary to minimise the duration of the FT campaign as recorded data can be analysed by an Engineer post-manoeuvre to determine if a satisfactory data set has been recorded. Another requirement for accurate model identification relates to the pertinent issue of in-flight adaptive and reconfigurable flight control. Research into improved fault-tolerance has also been central to the development of online aircraft SysID; examples of which include Chandler *et al* [2] and Ward *et al* [3] that address the complex issue of dealing with data from non-manoeuvering flight. Other uses address the the need to develop good aerodynamic databases for flight simulator models, [4], however, such tests tend to be performed to demonstrate a proof-of match and therefore do not depend on a real-time capability.

1.1 Aircraft System Identification

A brief explanation of key points relating to the process of aircraft SysID will now follow, an in-depth explanation can be found in Klein [5]. The conventional method is shown in figure 1, the process requires, *a priori* knowledge of the aircraft and then follows five distinct steps: experiment design, Data Compatibility Check (DCC), model structure determination, parameter estimation and model validation.

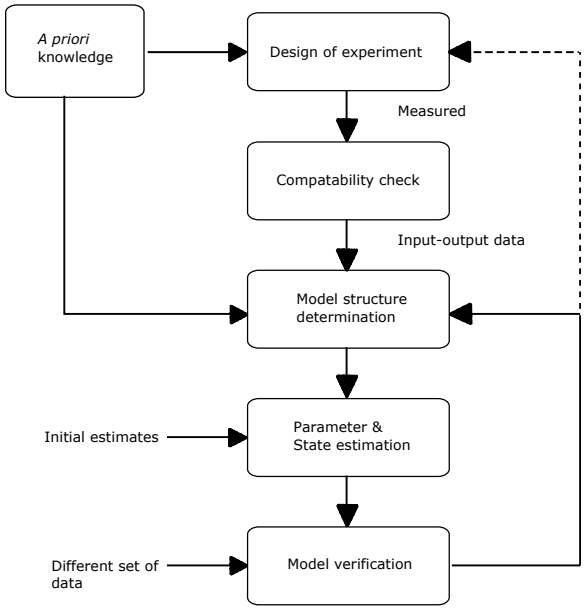

Fig. 1 An overview of the SysID process, [6].

The experiment design relates to the type of input used to perturb the aircraft from the steady level flight condition, defined as *trim*. Following this the DCC processes the data to estimate gross errors, data drop-outs and ensure kinematic consistency. In certain cases the model structure for the aircraft is then determined from the data, the

model is then populated with the estimated model parameters and states. Finally, the representative model is validated by using a separate data set not previously used during the model identification process. Should a validation fail, an alternative input is then selected and the identification process repeated (represented by the dotted line in figure 1). In the research presented the data was already known to be compatible therefore the DCC was ignored and the SysID process proceeded directly to the Parameter Estimation (PE) step. Using *a priori* knowledge of the aircraft reduced order models for the SPPO mode were postulated. Such simplifications enabled the investigation to focus on the effect of noise in the measured data on the parameter estimation step.

1.2 Paper outline

The aim of the current work is to develop a portable real-time tool-box capable of performing post-manoeuvre parameter estimation for postulated reduced order SPPO, Dutch Roll and Roll mode models. The primary benefits of creating the portable tool-box will include: a reduction in time taken to process/analyse data and a reduction in costs of having to repeat FT points (FT data is made available on an opportunistic basis when an aircraft is flown for research purposes). In order to achieve this reliable low noise data needs to be obtained, however, this is dependent on the quality of the instrumentation used and the amount of atmospheric turbulence present during the test. As a result an investigation into suitable filtering/smoothing techniques before differentiation under the constraints of post-manoeuvre performance was conducted using methods developed and presented by Klein and Morelli [7]. Data from two sources were analysed; firstly flight test data from the University Jetstream-31 (G-NFLA) which operates as a flying classroom, and secondly, data from the Aerosonde UAV in the Simulink simulation environment. This paper is divided into 5 sections, section 2 outlines the methodology implemented to process and collect the data, section 3 presents the Jetstream SysID results followed by discussion, the Aerosonde results and discussion then follow in section 4 before the paper is concluded with the key findings and future work outlined in section 5

2 Method

A key aspect in accurate SysID is the quality of the recorded data. Primary contributors to signal noise include: instrument and sensor errors, poor instrument isolation from aircraft vibrations, and atmospheric turbulence. In the case of smaller UAV's not all the required parameters can be recorded accurately or at all [8]. In addition, an appropriate choice of excitation input is also necessary to provide a sufficient signal capable of being detected above the noise. For the Equation Error (EE) parameter estimation technique angular accelerations such as $\dot{p}$, $\dot{q}$ and $\dot{r}$ are needed and are usually determined by differentiation of the measured angular rates p, q and r [1].

Before progressing the differences between filtering and smoothing should be outlined [7]. Filtering, at a given point in time, uses the previous data points up to and including the current point to remove noise from a signal. In contrast smoothing is performed using future and past data points along with the current data point and therefore can only be performed once the complete data set is available. Filtering is the only option for strict real-time applications. However, in the case of post-manoeuvre data processing the full data set is available and smoothing may be performed.

2.1 Local polynomial fitting

An analytical time domain method for obtaining smoothed derivatives is proposed by Klein and Morelli [7] where a local quadratic least squares fit of the data points is differentiated. Each data point along with the four nearest neighbouring ones are used to form the local quadratic. However, at the end points there are insufficient data points, which require the equation to be modified accordingly. The equations to be solved are:

$$
\begin{aligned}
z_1 =& \frac{1}{70\Delta t}\left[-54z_1 + 13z_2 + 40z_3 + 27z_4 - 26z_5\right] \\
z_2 =& \frac{1}{70\Delta t}\left[-34z_1 + 3z_2 + 20z_3 + 17z_4 - 6z_5\right] \\
z_{3:n} =& \frac{1}{10\Delta t}\left[-2z_{1:n-4} - z_{2:n-3} + z_{4:n-1} + 2z_{5:n}\right] \\
z_{n-1} =& \frac{1}{70\Delta t}\left[34z_n - 3z_{n-1} - 20z_{n-2} - 17z_{n-3}\right. \\
& \left. + 6z_{n-4}\right] \\
z_n =& \frac{1}{70\Delta t}\left[54z_n - 13z_{n-1} - 40z_{n-2} - 27z_{n-3}\right. \\
& \left. + 26z_{n-4}\right]
\end{aligned} \tag{1}
$$

where Δt is the sampling interval in seconds, and *n* is the number of data points, equal to the length of the data to be differentiated.

2.2 Global Fourier smoothing

An alternative method to the local time domain smoothing and differentiation is the more advanced automatic global Fourier smoothing developed by Morelli [9], which analyses the complete data set in the frequency domain before differentiation. Fourier sine series describing the measured data are calculated and from analysis of the principal spectral components the deterministic component of the signal can be distinguished from that of the random noise. In order to smooth the high frequency noise automatically analytical models of the signal and noise need to be determined. These are necessary to determine the optimal filter known as a Wiener filter. Smoothing is then achieved by the product of the data and filter. Once obtained the smoothed data is differentiated. For the purposes of clarity only an overview of the automatic global Fourier smoothing equations are presented, the interested reader is directed to Morelli [9] for further information regarding the analytical signal and noise models.

The Fourier transform assumes that the time history is periodic, therefore the start and end points of the data need to be removed by subtracting a linear trend from the data, $z(i)$ before reflecting the data about its origin:

$$
g(i) = z(i) - z(1) - (i-1)\left[\frac{z(n) - z(1)}{n-1}\right] \tag{2}
$$

where $i = 1, 2 \ldots n$. The vector can then be approximated by a Fourier sine series as it is an odd function of time without the end point discontinuities:

$$
\hat{g}(i) = \sum_{k=1}^{n-1} \boldsymbol{b}(k) \sin\left[k\left(\pi\frac{i-1}{n-1}\right)\right] \tag{3}
$$

where $\boldsymbol{b}(k)$ are the Fourier sine series coefficients given by:

$$
\boldsymbol{b}(k) = \frac{2}{n-1}\sum_{k=2}^{n-1} g(i) \sin\left[k\left(\pi\frac{i-1}{n-1}\right)\right] \tag{4}
$$

where the discrete frequency index, $k = 1, 2 \ldots n-1$. The Wiener filter $\boldsymbol{\phi}(k)$ is obtained from analytical models of the signal, Y and noise, N, of the Fourier sine series coefficients [9]:

$$
\boldsymbol{\phi}(k) = \frac{Y^2(k)}{Y^2(k) + N^2(k)} \tag{5}
$$

A example showing plots for the signal and noise models used to determine the cut-off frequency, f_c is illustrated in figure 2. The shape of the filter, $\Phi(k)$ in figure 3 is given by equation 5, the location of the inflection at $\Phi = 0.5$ is dependent on the data and is equal to the cut-off frequency, f_c. The Fourier smoothed signal is then obtained

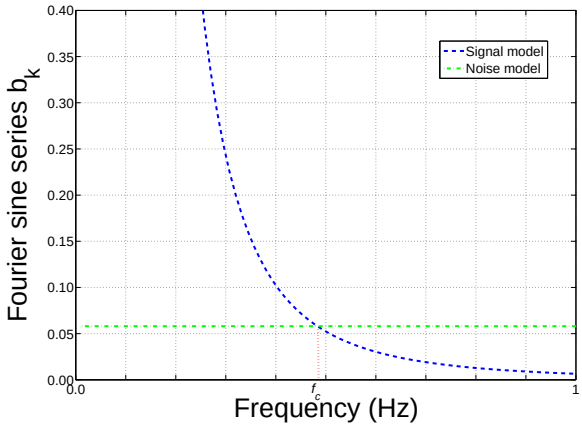

Fig. 2 Signal spectral content example

by multiplying the Wiener filter and Fourier sine series:

$$
\hat{g}_s(i) = \sum_{k=1}^{n-1} \boldsymbol{\phi}(k)\boldsymbol{b}(k) \sin\left[k\left(\pi\frac{i-1}{n-1}\right)\right] \tag{6}
$$

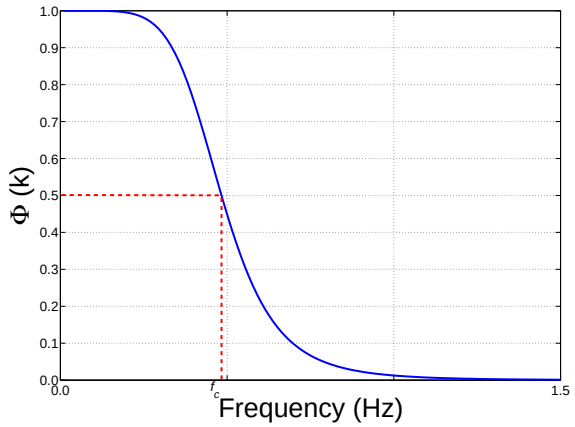

Fig. 3 Wiener filter example

finally the linear trend removed from the data is restored and the Fourier smoothing is complete:

$$\boldsymbol{z}_s(i) = \hat{g}_s(i) + z(1) + (i-1)\left[\frac{z(n) - z(1)}{n-1}\right] \quad (7)$$

Now the smoothed signal can be differentiated with respect to time, yielding:

$$\dot{\boldsymbol{z}} = \left[\frac{z(n) - z(1)}{n-1}\right] + \sum_{k=1}^{n-1} \boldsymbol{\phi}(k)\boldsymbol{b}(k)\left(\frac{k\pi}{n-1}\right)\cos\left[k\pi\left(\frac{i-1}{n-1}\right)\right] \quad (8)$$

2.3 Equation Error method

In considering the real-time nature of the proposed tool box, methods that are iterative such as the Maximum Likelihood estimation technique [10] need to be avoided. A non-iterative technique that has been successfully applied to FT data is the Equation Error (EE) technique that estimates the parameters by using an ordinary least squares regression, [5]. Re-arranging the equations of motion into state space form, in which dependent variables y are equal to the product of the unknown parameters, $\boldsymbol{\theta}$ and their regressors $\boldsymbol{X}$ yields:

$$y(t) = \theta_0 + \theta_1 X_1(t) + \theta_2 X_2(t) \ldots + \theta_n X_n(t) \quad (9)$$

In order to account for the error, equation 9 is modified to become the measurement equation:

$$z(i) = y(i) + \epsilon(i) = \theta_0 + \sum_{i=0}^{n} \theta_j X_j(i) + \epsilon(i), \quad i = 1, 2 \ldots n \quad (10)$$

placing equation 10 in matrix form:

$$\boldsymbol{z} = \boldsymbol{X\theta} + \boldsymbol{\epsilon} \quad (11)$$

and assuming that the error, $\boldsymbol{\epsilon}$ can be represented as white noise with zero mean and variance: $E[\boldsymbol{\epsilon}] = \boldsymbol{0}$ and $E[\boldsymbol{\epsilon\epsilon}^T] = \sigma^2\, \boldsymbol{I}$ allows the least squares approach to be applied. Therefore, re-arranging equation 11 yields the unknown parameters $\boldsymbol{\theta}$, [11]:

$$\hat{\boldsymbol{\theta}} = (\boldsymbol{X}^T\boldsymbol{X})^{-1}\boldsymbol{X}^T\boldsymbol{z} \quad (12)$$

2.4 Reduced order models

From *a priori* knowledge, the standard rigid body equations of motion can be used to formulate a model which should adequately describe the aircraft dynamics. One assumption when using such models is that the longitudinal and lateral dynamics can be decoupled. The following body axes SPPO model taken from Cook [12] was used for this study:

$$\begin{bmatrix}\dot{\boldsymbol{W}} \\ \dot{\boldsymbol{q}}\end{bmatrix} = \begin{bmatrix} z_w & z_q \\ m_w & m_q \end{bmatrix}\begin{bmatrix}\boldsymbol{W} \\ \boldsymbol{q}\end{bmatrix} + \begin{bmatrix} z_\eta \\ z_\eta \end{bmatrix}[\boldsymbol{\eta}] \quad (13)$$

2.5 Signal to noise

When dealing with experimental data it is useful to know the Signal to Noise Ratio (SNR), which provides quantification of how much a signal has been corrupted by noise. The ratio is given by the logarithmic equation:

$$SNR = 20\log_{10}\left(\frac{P_{signal}}{P_{noise}}\right) \quad (14)$$

where P_{signal} and P_{noise} represent the root mean square power values:

$$P_x = \sqrt{\frac{x^T \times x}{n}} \quad (15)$$

where x is the data either for the deterministic part of the signal or the noise and n is the length of the data.

2.6 Excitation inputs

Several types of inputs have been developed in order to sufficiently excite the aircraft dynamics [13], [14]. The input used to excite the Jetstream was an impulse. Such a manoeuvre is used to demonstrate the SPPO mode and does not consist of a typical SysID input because it excites a limited range of frequencies. However, large data sets of the Jetstream aircraft are readily available.

Three inputs that are routinely used for system identification include: the doublet, a '3211' and a frequency sweep, these are shown in figure 4 and were applied to the Aerosonde UAV. Furthermore, as the Aerosonde example was a simulation this enabled a perfect data set to be reproduced, which poses a problem for model validation. However, by using a different input such as the boxcar input (figure 5) the pitch rate response from simulation could be compared with the predicted pitch rate responses from the three models determined using the different excitations.

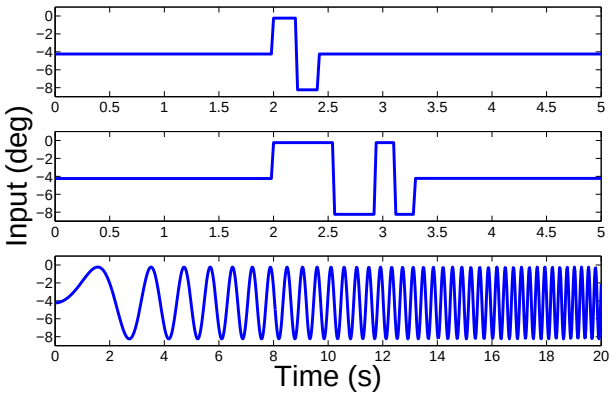

Fig. 4 Sample types of excitation inputs

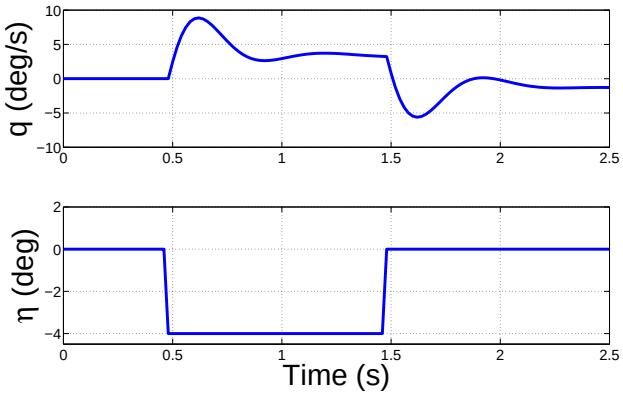

Fig. 5 Aerosonde model validation input

3 Jetstream investigation

Fig. 6 Cranfield's Jetstream-31 G-NFLA

The BAe Jetstream-31 is a successor to the Handley Page HP-137 designed in 1965 as a passenger aircraft capable of carrying 18 passengers at a cruising speed of 230 kts (at 25,000ft) with a maximum range of 680 nm (1260 km) and MTOW 6,950 kg. In its current guise (figure 6) the aircraft provides Cranfield University with an instrumented flying laboratory used to demonstrate the principles of flight dynamics to students. The aircraft's role as a flying laboratory requires that excitation inputs suitably demonstrate the dynamic modes, in the case of the SPPO mode an impulse input is used. However, due to the fact that copious data records are readily available the Jetstream is a useful source for the purposes of investigating aircraft SysID. Onboard instrumentation such as the inertial measurement unit, accelerometers and α-vane provide the required regressors for the EE method (section 2.3). Furthermore, the recorded data is pre-filtered onbord by a hard-wired filter (a low pass second order butterworth filter) with a cut-off frequency of 8Hz.

3.1 Results Jetstream

The results presented below are for the following flight condition: V_{TAS} = 173 kts (89 m/s), altitude = 6080 ft (1853.2 m) and a c.g. of 23 % MAC. Applying the global Fourier smoothing, the Fourier series for the pitch rate are shown in figure 7 along with the signal and noise models required to calculate the Weiner filter (equation 5). The SPPO model parameter estimates for both methods are presented in table 1. Finally, the pitch rate response for the two models' validated using a seperate set of data are included in figure 8.

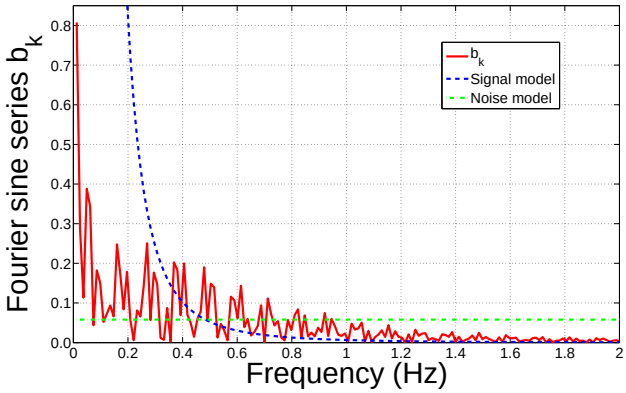

Fig. 7 Signal spectral content: Jetstream impulse

$\hat{\theta}$	Global	s	Local	s
z_w	-0.232	0.172	-0.862	0.065
z_q	24.290	4.411	79.525	2.084
z_η	-17.550	5.274	-0.831	3.210
m_w	-0.054	0.010	-0.071	0.011
m_q	0.445	0.294	0.381	0.345
m_η	-2.014	0.359	-5.072	0.685

Table 1 Derivatives and standard errors: Jetstream

3.2 Discussion Jetstream

Referring to figure 7 the frequency content in the measured data for the impulse elevator deflection is shown. The high peaks present at low frequencies (0 - 0.1Hz) indicate that the excitation was insufficient to provide large Fourier coefficients over a wider frequency bandwidth.

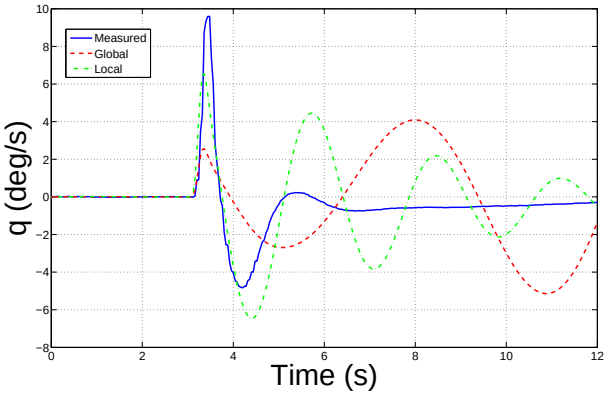

Fig. 8 Pitch rate response: Jetstream validation

This resulted in a low cut-off frequency, equal to 0.48Hz. Which excluded several smaller peaks that occured up to approximately 1Hz.

Comparing the estimated parameters for both methods (see table 1), significant differences occur for the values of z_q, z_η and m_η parameters. Furthermore, the m_q estimates were both positive, explaining the predicted models' oscillatory behaviour this may have been caused due to differentiation of the *w* and *q* data. However, the local method's predicted pitch rate showed light damping and can be explained due to the greater magnitude of z_w. Identified models from both smoothing techniques were unable to capture the true aircraft SPPO dynamic response. The SNR value for the pitch rate response was calculated to be 6.20 as opposed to the higher value of 13 for the Aerosonde discussed in the next section. Therefore, some of the error for the parameter estimates of the Global smoothing method can be attributed to the low signal information content due the use of an impulse excitation. Previous work has shown that replacing differentiation of the measured variable *w* with $\dot{w}$ results in a better model identification [8].

The validation of SysID results, produced poorly damped responses for both smoothing methods (figure 8). The Global method response exhibited a highly oscillatory response. In comparison, the Local method better predicted the initial response (T = 3 to 4 s), before exhibiting a lightly damped oscillation.

4 Aerosonde investigation

The Aerosonde UAV is a small aircraft (*b* = 2.9 m) designed primarily for weather-reconnaissance and remote-sensing missions, it has a twin tail boom with a rear mounted pusher propeller configuration with a speed range of 40 - 60 kts and a MTOW of 15kg (figure 9). Using the simulation environment enables further analysis to be focused on specific aspects, such as the effect of varying perturbation inputs. Therefore, the effect of varying the input excitation for representative sensor noise was investigated using a Simulink model. The flight condition used was V_{TAS} = 44.7 kts (23 m/s), altitude = 3281 ft (1000 m) and a c.g. of 15 % MAC. Standard white noise was generated using the associated Simulink block and added to the required regressor measurements. Noise power was set at: gyroscope = 2.75×10^{-6}, accelerometer = 2.5×10^{-4}, α and β-vanes = 2×10^{-8} and pitot, (V_{EAS}) = 1×10^{-6}. The three types of excitation inputs described in section 2.6 were applied to the elevator.

Fig. 9 The Aerosonde UAV [15]

4.1 Results Aerosonde

Strip plots of the pitch rate and elevator input data used in the analysis for the three different cases are shown in figures 10 to 12 with their *trim* values removed. The Global smoothing method's Fourier sine coefficients, signal and noise models are plotted against frequency in figures 13 to 15. The parameter estimates for both methods are shown in tables 2 to 4. Using the Linmod Matlab function linearised parameters for the Aerosonde Simulink model were extracted for comparison with the estimated parameters, and these are included in the first column of each table. Finally, the validation pitch rate responses are presented in figures 16 to 18.

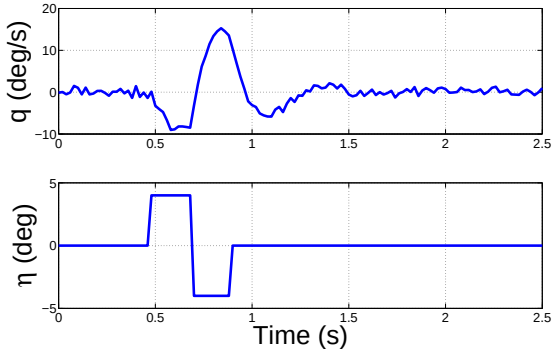

Fig. 10 Aerosonde doublet

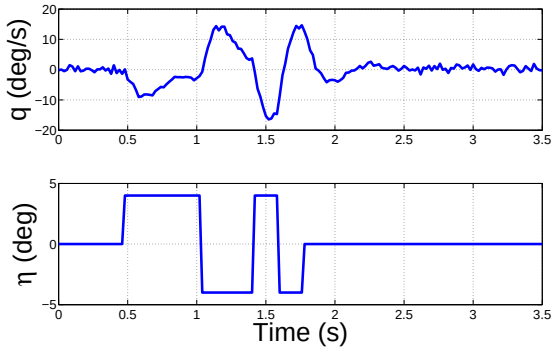

Fig. 11 Aerosonde '3211'

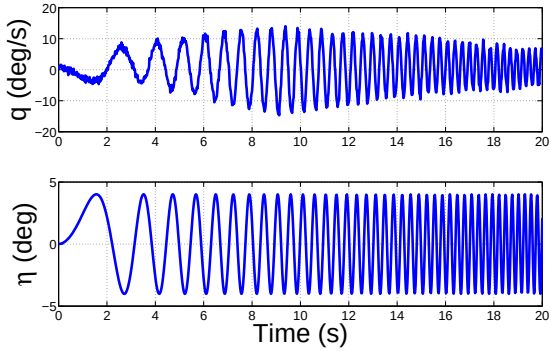

Fig. 12 Aerosonde frequency sweep

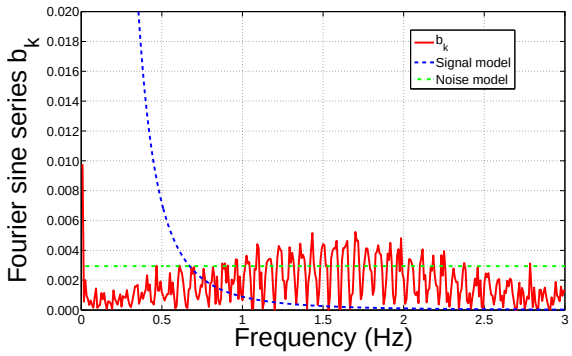

Fig. 13 Signal spectral content: Aerosonde doublet

$\hat{\theta}$	Lin	Global	s	Local	s
z_w	-4.115	-0.059	0.139	-3.940	0.303
z_q	24.30	0.356	0.330	19.623	0.945
z_η	-2.343	0.188	0.898	-2.890	2.365
m_w	-4.289	$-3.0e^{-4}$	0.001	-5.116	0.170
m_q	-6.027	$8.0e^{-4}$	0.001	-3.354	0.668
m_η	-32.45	0.002	0.004	-23.790	1.752

Table 2 Derivatives and standard errors: Aerosonde doublet

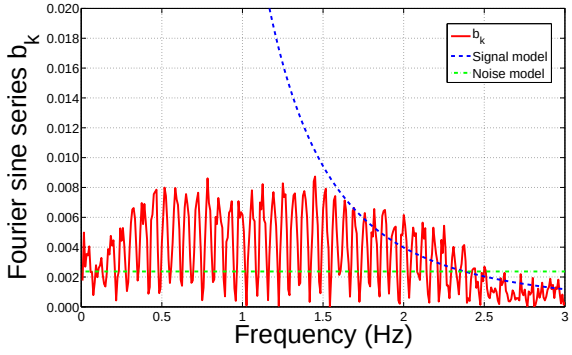

Fig. 14 Signal spectral content: Aerosonde '3211'

$\hat{\theta}$	Lin	Global	s	Local	s
z_w	-4.115	-3.048	0.456	-3.856	0.179
z_q	24.30	16.854	1.670	20.652	0.663
z_η	-2.343	-1.227	3.429	-2.955	1.612
m_w	-4.289	-4.067	0.268	-4.515	0.151
m_q	-6.027	-1.782	0.882	-4.121	0.594
m_η	-32.45	-17.359	1.981	-25.592	1.521

Table 3 Derivatives and standard errors: Aerosonde '3211'

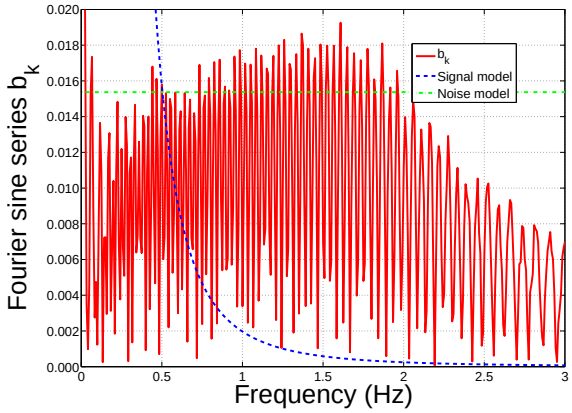

Fig. 15 Signal spectral content: Aerosonde frequency sweep

$\hat{\theta}$	Lin	Global	s	Local	s
z_w	-4.115	-0.037	0.054	-3.847	0.083
z_q	24.30	0.193	0.109	20.640	0.252
z_η	-2.343	0.029	0.333	-2.782	0.600
m_w	-4.298	0.091	0.119	-4.587	0.028
m_q	-6.027	0.005	0.388	-5.555	0.104
m_η	-32.45	0.799	0.891	-30.620	0.254

Table 4 Derivatives and standard errors: Aerosonde Frequency sweep

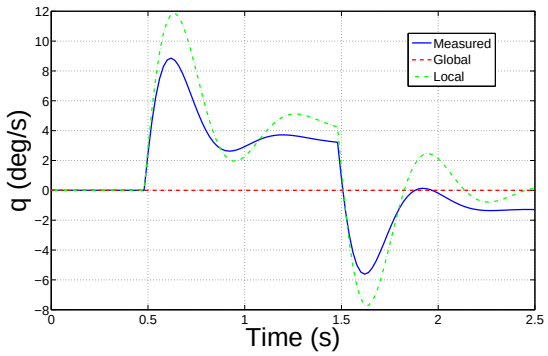

Fig. 16 Pitch rate response: Aerosonde doublet

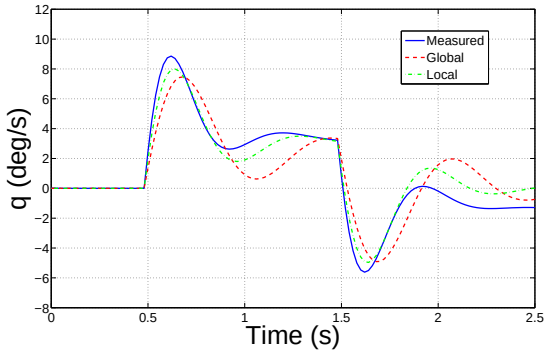

Fig. 17 Pitch rate response: Aerosonde '3211'

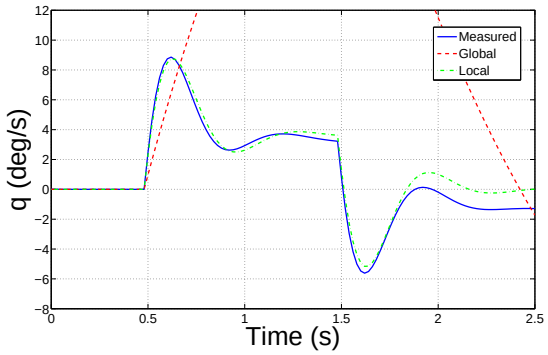

Fig. 18 Pitch rate response: Aerosonde frequency sweep

4.2 Discussion Aerosonde

Analysing the Global method results, the spectral frequency plots show that large Fourier sine coefficients are present at low frequencies (0 - 0.1 Hz) for the doublet and frequency sweep. However, such large coefficients are not visible in the '3211' plot, figure 14. As a result the f_c determined using the Global method for the doublet and frequency sweep occurs at 0.67 Hz and 0.48 Hz respectively. In contrast, the '3211' f_c equals 2.43 Hz, resulting in more information from the measured signal being recovered. Comparing the SNR values for the pitch rate data, the doublet and '3211' values were close, 14.0 and 13.46 respectively with the frequency sweep yielding a lower value of 5.11. However, the large doublet SNR did not produce good results due to the large initial Fourier coefficient peak (figure 13) responsible for the low f_c. On comparison of the parameter estimates under the Global column with the linearised values both the doublet and frequency sweep parameters (tables 2 and 4) are significantly smaller than the reference linearised values. The '3211' parameters follow the linearised values well, with distinguishable differences for z_w, z_q, m_q and m_η. Furthermore, the corresponding pitch rate validation plots for the doublet and frequency sweep underline the effect of the Global method selecting too low a f_c for the doublet and frequency sweep.

Referring to the parameter estimates listed under the Local column and comparing them with the linearised model values the doublet and '3211' parameters are of the same magnitude and sign. However, the closest match is achieved by the frequency sweep parameter estimates along with the lowest overall standard errors, highlighted by the pitch rate response figure 18. The largest differences between parameter estimates were the same for the three inputs and occured for the z_q, m_q and m_η parameter estimates. It must be stated that some of the differences between the estimated and linear parameters can be accounted for by the fact that the linearised model has 6 degrees of freedom in comparison to the reduced order model.

Overall the '3211' method was found to be best suited to sufficiently excite the Simulink model over a wider frequency bandwidth. In addition, the Local smoothing method provided the most consistent results for the three types of inputs used.

5 Conclusions and Further work

An investigation into the performance of two different smoothing techniques applied to flight test and simulated data before differentiation has been performed. Using the EE method parameter estimates for the reduced order SPPO models for the BAe Jetstream-31 aircraft and a simulated Aerosonde UAV were obtained.

For the global Fourier smoothing method the results were affected by the type of input used to excite the aircraft, which changed the signal to noise ratio. In addition, the best results were achieved when the perturbation to the aircraft produced low Fourier coefficients at low frequencies. This highlighted the method's sensitivity to large Fourier peaks which subsequently effected the value of f_c. Overall, it was found that the local polynomial smoothing method provided the best results for both aircraft. For the simulation case the '3211' excitation input provided comparable results between the two methods, as it enabled frequency content to be spread across the bandwidth. However, the closest match was achieved using the frequency sweep and the Local method.

Following the current findings, the Local polynomial method would be best suited for the development of a post-manoeuvre tool-box using differentiation to determine the regressors. However, previous work has been performed using reconstruction as an alternative to overcome the additional error incurred when differentiating. Furthermore, analysis of the two smoothing techniques could be expanded to consider the lateral modes: Dutch Roll and Roll. Finally, having gained an understanding for the near real-time constraints future work will need to address the issue of a real-time application, where smoothing is not possible and needs to be replaced by filtering.

Acknowledgments

This research is funded by a CASE award supported jointly by EPSRC and BAe Systems. The author would like to thank Dr A. K. Cooke for his supervision and approachability and Dr S. D. Carnduff for his time and informative discussions.

References

[1] S. D. Carnduff. *"System identification of Unmanned Aerial Vehicles"*. Phd thesis, Cranfield University, Cranfield, Bedfordshire, 2008.

[2] M. Prachter P.R.Chandler and M. Mears. "System identification for adaptive and reconfigurable control". *Journal of Guidance, Control, and Dynamics*, Vol 18 (3):pp 516–524, May - June 1995.

[3] J.F. Monaco D. G. Ward and M. Bodson. "Development and flight testing of a parameter identification algorithm for reconfigurable control". *Journal of Guidance, Control and Dynamics*, Vol 21 (6):pp 948–956, November - December 1998.

[4] R. Jategaonkar. *"Flight Vehicle System Identification: A Time Domain Methodology"*. AIAA, Reston, Virginia, 2006.

[5] V. Klein. "Estimation of aircraft aerodynamic parameters from flight data". *Progress in Aerospace Sciences*, Vol 26 (1):pp 1–77, 1989.

[6] V. Klein. "A review of system identification methods applied to aircraft". Technical Report Joint Institute for Acoustics and Flight Sciences Report: N83 33901, The George Washington University, 1983.

[7] V. Klein and E. A. Morelli. *"Aircraft System Identification: Theory and Practice"*. AIAA, Reston, Virginia, 2006.

[8] P-D. Jameson and A.K. Cooke. "Devloping system identification for uavs". In *25th Bristol International UAV Systems Conference*, Bristol, United Kingdom, 12 - 14 th April 2010.

[9] E. A. Morelli. "Estimating noise chracteristics from flight test data using optimal fourier smoothing". *Journal of Aircraft*, Vol 32 (4):pp 689–695, July - August 1995.

[10] K. W. Iliff. "Parameter estimation for flight vehicles". *Journal of Guidance, Control, and Dynamics*, Vol 12:pp 609–622, September - October 1989.

[11] L. Ljung. *"System Identification: Theory for*

the user 2nd editon". Prentice Hall PTR, New Jersey, 1999.

[12] M. V. Cook. *"Flight Dynamic Principles : A linear systems approach to aircraft stability and control"*. Elsevier, Amsterdam, 2007.

[13] J. A. Mulder. *"Design and evaluation of dynamic flight test manoeuvers"*. Phd thesis, Delft University of Technology, Delft, 1986.

[14] E. A. Morelli. *"Practical input optimisation for aircraft parameter estimation experiments"*. Phd thesis, George Washington University, Washington, DC, 1990.

[15] *Photo Aerosonde, Atlantic 1998, Wallpaper free for common use, taken from Aerosonde Pty Ltd*. www.aerosonde.com, 11/04/2005.

6 Copyright Statement